

Prediction and Analysis of Global Temperature Based on BP and ELMAN Neural Networks

Xiuyang Wu, Yuwen Wang, Xiaoxian Zhang

School of Science, China University of Petroleum, Beijing, 102249, China

Abstract: *In order to explore the global climate evolution and change patterns, this article uses global temperature data from 1881 to 2020 for nearly 140 years, and based on the global temperature zone division model, constructs BP neural network and ELMAN neural network prediction models to analyze the spatiotemporal evolution trend of global temperature historical data. It is found that the average temperature in the northern and southern hemispheres began to significantly increase around 1950; based on the above model, it is predicted that the global annual average temperature will reach its peak around 2050 and continue to maintain around 16.6433°C for the next fifty years.*

Keywords: *global temperature changes, BP neural network, ELMAN neural network, forecast*

1. Introduction

The latest report released by the World Meteorological Organization points out that the average temperature in the European region increased by 0.5 degrees Celsius every ten years between 1991 and 2021^[1]; The sixth assessment report issued by the Intergovernmental Panel on Climate Change (IPCC) also warned that the average global surface temperature in 2011-2020 increased by 1.1°C compared with 1850-1900^[2]. Throughout the past century, both the northern and southern hemispheres have shown a significant upward trend in Earth's temperature.

Over the past half century, significant global warming has become an important issue for sustainable development of human economy and society, attracting widespread attention from various sectors. Some studies have found that since the 1980s, it has been the period with the fastest rate of global land temperature rise^[3], but some scholars believe that global warming has stagnated since the 21st century^[4]. Therefore, in order to better understand the global temperature changes since the beginning of the 21st century, we selected 20 cities globally based on the distribution of the Earth's temperature belt and collected temperature data from September 2003 to November 2022. By establishing a mathematical model of global average annual temperature and spatiotemporal changes, we conducted regression analysis and prediction, aiming to explore the potential laws of global temperature change and predict the future trend of global temperature change, in order to promote China's "dual carbon" strategy Provide scientific guidance for actively addressing climate change and mitigating global warming.

2. Prediction model

2.1 Linear regression prediction model based on BP neural network

The BP neural network with strong learning ability and easy operation is manifested as a topological structure, which processes information by constructing a unit layer similar to the synaptic structure of the brain. It is mainly composed of three layers: input, hidden, and output. The hidden layer is either single-layer or multi-layer, and the connection strength between unit layers is determined by additional weights between each layer. The use of BP neural networks to complete prediction tasks is mainly achieved through steps such as training samples, adjusting network parameters, and comparing prediction errors.

The algorithm logic of the BP neural network is: initialization of the BP network → calculation of the output value of the hidden layer according to the weights and neuron thresholds between layers → calculation of the output value of the output layer → calculation of the Mean squared error → continuous updating of the weights and thresholds → judgment. If the results meet the accuracy

requirements, the iteration will end^[5].

The BP neural network has strong nonlinear fitting ability, and combined with linear regression, it can effectively predict time series data. The linear regression combination prediction model based on the BP neural network in this article is shown in Figure 1.

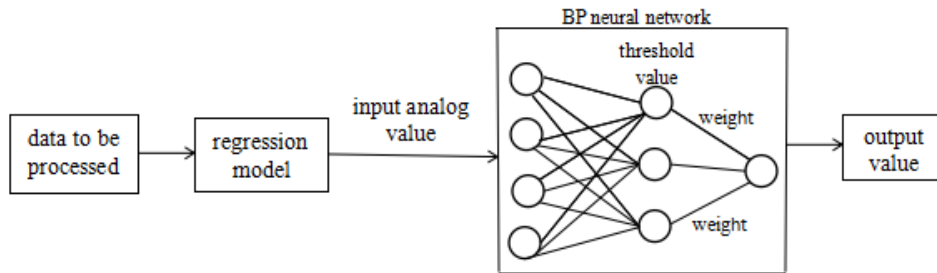


Figure 1: Linear regression prediction model based on BP neural network

2.2 Elman neural network temperature prediction model

The primary task of using an Elman neural network to predict temperature is to construct an Elman neural network and select appropriate input values. The output forms include single output, multi output, etc. The temperature prediction based on an Elman neural network only needs to output the temperature of a certain year in the future. Therefore, a single output form of the Elman neural network is chosen^[6]. The Elman neural network temperature prediction process is as follows: construct an appropriate Elman neural network structure → initialize input weights → normalize historical temperature sample data → calculate the output values of neurons, hidden layers, and connecting layers → use the adjusting weights of connecting layers for feedback. The prediction model and process based on Elman neural network are shown in Figure 2.

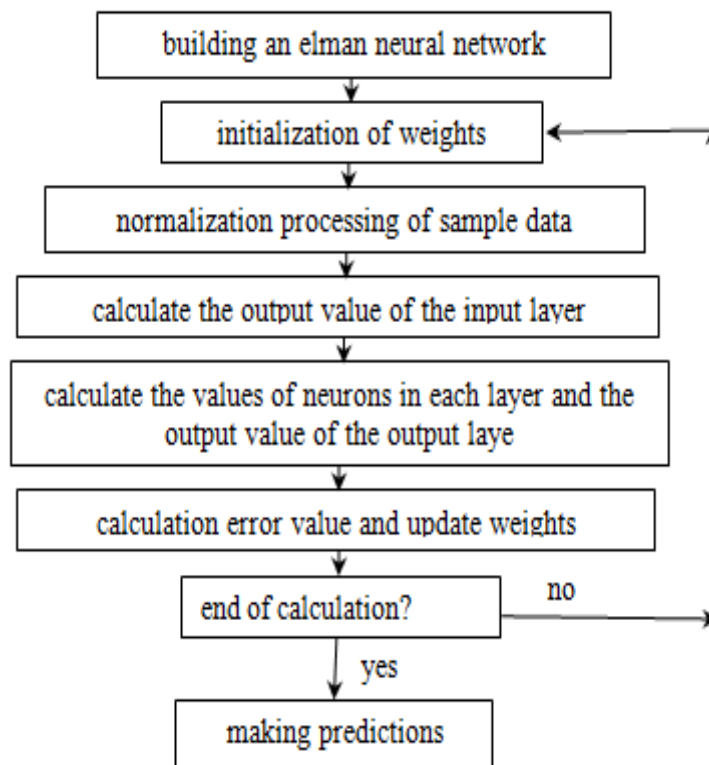


Figure 2: Elman neural network prediction model

3. Model Assumptions and Variable Explanation

3.1 Model Assumptions

The basic assumptions of the prediction model in this article mainly include:(a)within the prediction period, there will be no celestial body impact event that will affect the stability of the earth's ecosystem and the earth moon system;(b)the earth's plate does not move;(c)the collected data is authentic and reliable, meeting the basic requirements for data classification and analysis;(d)there will be no new serious factors affecting climate change in the next 100 years;(e)there will not be a huge breakthrough in human technology, and existing energy will still be the main focus^[7].

3.2 Variable Description

The variables involved in the prediction model in this article are mainly as follows (Table 1).

Table 1: Variable description

| variable symbol | meaning of variables |
|-----------------|---------------------------------|
| S_k | initial temperature time series |
| UF_k | trend statistics |
| $E(S_k)$ | order column mean |
| $Var(S_k)$ | rank sequence variance |

4. Data sources

To enhance the effectiveness of the data, this article collects historical spatiotemporal data of global temperature, with the statistical indicator set as average temperature. Due to the preliminary selection of 98 cities distributed in various temperate zones around the world and the complexity of climate types, based on the idea of "local mapping as a whole", in order to better reflect the spatiotemporal changes in global temperature trends, 20 representative cities were selected from 98 cities, and the selection of cities follows the following four main principles^[8].

4.1 Urban temperature is measured by average temperature

In the primary cities, the average temperature uncertainty fluctuates between 0.12 and 3.59, with an average of approximately 0.78. Therefore, the uncertainty of average temperature has a small impact on average temperature and can be ignored in classification analysis.

4.2 Cities evenly distributed in different temperature zones

According to latitude changes, the global temperature zone can be divided into five temperature zones: north south cold, temperate, and tropical. The climate temperatures of the same latitude in each temperature zone do not differ significantly at different longitudes, and the selected cities are roughly evenly distributed in different temperature zones around the world^[9].

4.3 Selected cities vary in latitude

Merge cities with the same latitude for statistics, and use the average temperature as the center value to represent the cities at that latitude, resulting in a collection of 49 cities with different latitudes.

4.4 The dimensional difference between adjacent cities is $\delta = 5^\circ$

49 cities are located in different temperature zones at different latitudes. For cities located in the same temperature zone, they are divided according to the latitude difference. Finally, 20 cities are selected as representative cities representing global temperature changes in different temperature zones (Table 2).

In addition, this article also retrieved temperature data from the NOAA official website for the

northern and southern hemispheres since 1881(Table3), and combined the two to obtain annual global average temperature data.

Table 2: 20 representative cities worldwide and their latitude and longitude

| Number | City | Country | Latitude | Longitude |
|--------|------------------|--------------|----------|-----------|
| 1 | Kabul | Afghanistan | 34.56N | 70.05E |
| 2 | Sydney | Australia | 34.56S | 151.78E |
| 3 | Dhaka | Bangladesh | 23.31N | 90.00E |
| 4 | Fortaleza | Brazil | 4.02S | 40.98W |
| 5 | Rio De Janeiro | Brazil | 23.31S | 42.82W |
| 6 | Salvador | Brazil | 13.66S | 38.81W |
| 7 | Rangoon | Burma | 16.87N | 95.44E |
| 8 | Montreal | Canada | 45.81N | 72.69W |
| 9 | Chongqing | China | 29.74N | 107.08E |
| 10 | Jinan | China | 36.17N | 117.35E |
| 11 | Shenyang | China | 40.99N | 123.55E |
| 12 | Bogotá | Colombia | 4.02N | 74.73W |
| 13 | Delhi | India | 28.13N | 77.27E |
| 14 | Madras | India | 13.66N | 80.09E |
| 15 | Baghdad | Iraq | 32.95N | 45.00E |
| 16 | Rome | Italy | 42.59N | 13.09E |
| 17 | Saint Petersburg | Russia | 60.27N | 29.19E |
| 18 | Durban | South Africa | 29.74S | 31.38E |
| 19 | Kiev | Ukraine | 50.63N | 31.69E |
| 20 | Harare | Zimbabwe | 18.48S | 30.42E |

Table 3: Temperature Data Table for the Northern and Southern Hemispheres

| Year | Month | Anomaly(south) | Year | Month | Anomaly(north) |
|-------|-------|----------------|-------|-------|----------------|
| 1881 | 5 | 0.065 | 1840 | 10 | -1.83 |
| 1881 | 6 | -0.852 | 1840 | 11 | -1.871 |
| 1881 | 7 | -0.598 | 1840 | 12 | -1.712 |
| 1881 | 10 | -0.208 | 1841 | 3 | -1.891 |
| 1881 | 11 | -0.552 | 1841 | 4 | -1.642 |
| 1881 | 12 | 0.089 | 1841 | 5 | -0.503 |
| 1882 | 1 | 0.279 | 1841 | 6 | -0.426 |
| 1882 | 2 | -0.065 | 1841 | 7 | 0.114 |
| 1882 | 3 | -0.371 | 1841 | 8 | -0.212 |
| 1882 | 4 | -0.784 | 1841 | 9 | -1.139 |
| 1882 | 5 | -0.355 | 1841 | 10 | -0.639 |
| 1882 | 6 | -0.922 | 1841 | 11 | -1.353 |
| 1882 | 7 | -0.737 | 1841 | 12 | -1.028 |
| | | | | | |

5. Model solving and analysis

5.1 Missing value interpolation

Individual missing data shall be interpolated by Linear interpolation method of adjacent stations to ensure good continuity of meteorological data after processing and correction.

According to the division of temperature bands, the average temperature data of repaired cities in the same temperature band is taken as the mean, representing the monthly historical spatiotemporal average temperature under that temperature band.

5.2 M-K mutation point test based on average temperature

Mann Kendall method is a non Parametric statistics test method. This test method does not require samples to follow the determined parameter distribution. It is applicable to type variables and sequence

variables, and highly praised by the World Meteorological Organization. The M-K test can be used for statistical testing of the above data, which helps to determine the mutation area and the time point at which the mutation begins^[10].

For a temperature time series with a sample size of n , the following rank sequence can be constructed first:

$$S_k = \sum_i^k r_i \quad (k = 2, 3, \dots, n) \tag{1}$$

In formula (1), S_k is the cumulative number of times when the temperature value in the i -th month is greater than the value in the j -th month, and there's also:

$$r_i = \begin{cases} 1, & x_i > x_j \\ 0, & x_i < x_j \end{cases} \quad (j = 1, 2, \dots, j) \tag{2}$$

When the temperature time series is a random sequence, the trend statistic U is:

$$UF_k = [S_k - E(S_k)] / \sqrt{Var(S_k)}, \quad (k = 1, 2, \dots, n) \tag{3}$$

In formula (3), $E(S_k)$ and $Var(S_k)$ are the mean and variance of the rank sequence respectively, when the temperature time series are independent of each other, $E(S_k)$ and $Var(S_k)$ are respectively:

$$E(S_k) = \frac{k(k-1)}{4}, Var(S_k) = \frac{k(k-1)(2k+5)}{72}, (2 \leq k \leq n) \tag{4}$$

Generally, UF_k is the standard Normal distribution, when given significance test level $\alpha = 0.05$, looking up the table, it was found that $U\alpha = \pm 1.96$, if $U\alpha < UF_k$, it proves that the temperature time series has a clear trend of change. If the values of UF_k and UB_k are both greater than 0, so it indicates an upward trend in the temperature time series, while the opposite indicates a downward trend. When the values of UF_k and UB_k both exceed the critical line, indicating a significant upward or downward trend in temperature time series; if UF_k and UB_k intersect between critical lines, this point is the mutation point of the temperature time series, so the corresponding time is the time when the temperature mutation begins^[11].

Based on the above theories and models, using Matlab software, the average monthly temperature changes and M-K test results of the four temperature zones of southern temperate zone, southern tropical zone, northern temperate zone, and northern tropical zone can be obtained (Figure 3 to Figure 10).

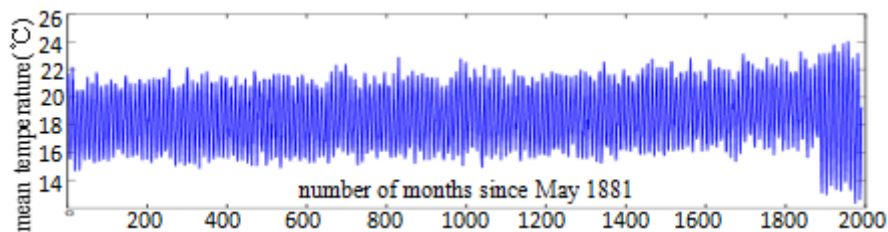


Figure 3: Mean monthly temperature in the south temperate zone

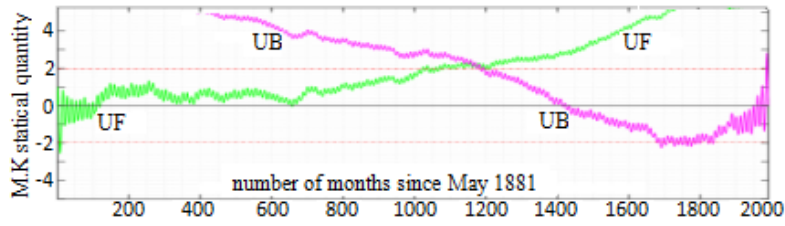


Figure 4: M-K statistical chart of mean monthly temperature in the south temperate zone

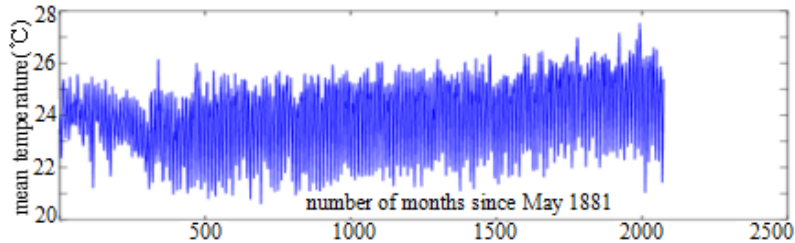


Figure 5: Mean monthly temperature in the southern tropics zone

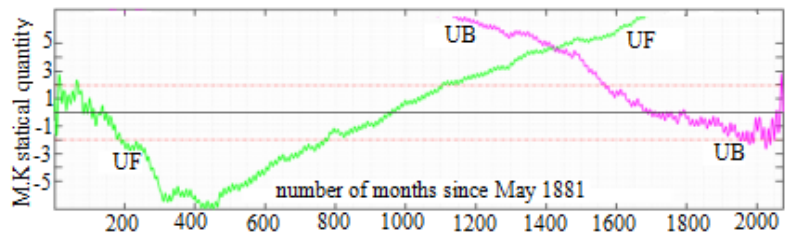


Figure 6: M-K statistical chart of mean monthly temperature in the southern tropics zone

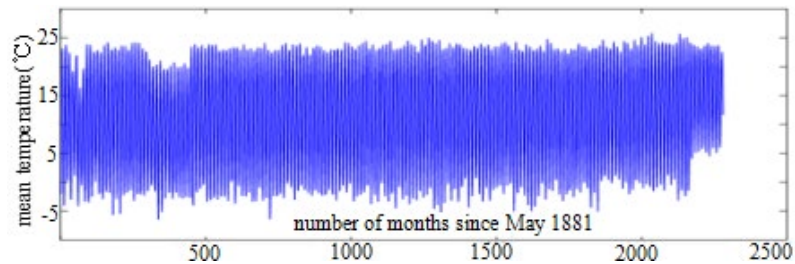


Figure 7: Mean monthly temperature in the north temperate zone

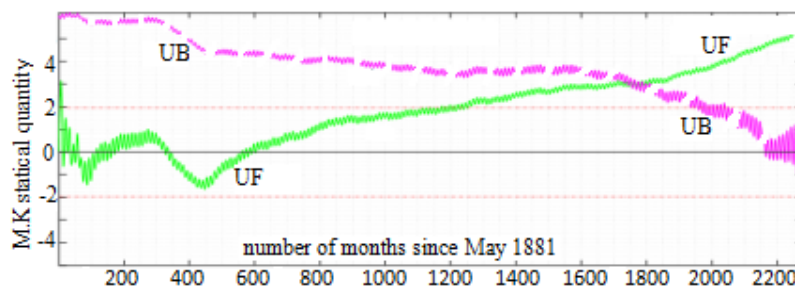


Figure 8: M-K statistical chart of mean monthly temperature in the north temperate zone

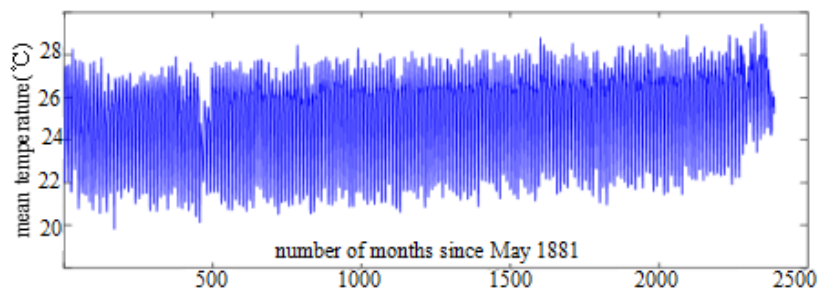


Figure 9: Mean monthly temperature in the north tropic zone

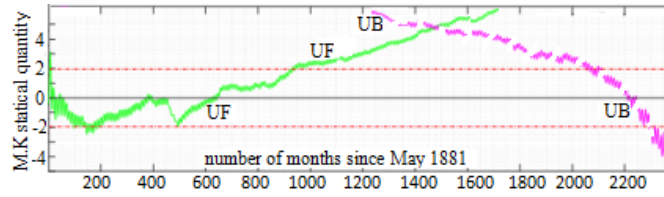


Figure 10: M-K statistical chart of mean monthly temperature in the north tropic zone

5.2.1 Analysis of spatiotemporal temperature change trend based on the average temperature change chart

Based on the average monthly temperature changes and trends of the four temperature zones mentioned above, it can be seen that the trend of monthly temperature changes is stable, indicating a high degree of stability in global spatiotemporal temperature data. Among them, the extreme values of the southern tropical and southern temperate zones differ greatly around the 21st century, with severe fluctuations, indicating frequent extreme weather events in that time and space^[12].

5.2.2 Trend and mutation point analysis based on M-K test chart

The comparative analysis of M-K statistical results for the four temperature zones mentioned above is as follows (Table 4).

Table 4: M-K Statistical Results for Each Temperature Zone

| | the south temperate zone | southern tropics | the north temperate zone | north tropic |
|-------|--------------------------|------------------|--------------------------|--------------|
| value | 2.18262 | 4.48715 | 3.0622 | 4.84857 |
| time | 1947-07-01 | 1969-09-01 | 1997-02-01 | 1973-09-01 |

From all UF and UB values greater than 0, it can be seen that temperatures in various temperature regions around the world are showing an upward trend, and the years of temperature sudden changes are concentrated in the second half of the 20th century, while global temperature changes will tend to stabilize in the 21st century^[13].

5.2.3 Global average temperature analysis based on BP neural network

When using BP neural network to analyze global average temperature, the following settings must be made in the training interface of Matlab software:(a) Set the division method of sample data as random division; (b) Levenberg Marquardt algorithm is used to train sample data; (c) Mean squared error is used to measure the performance of the network; (d) Set the target accuracy to 0.001.

According to the error formula, the error results of the BP neural network model with 4 hidden layer nodes are calculated as follows (Table 5).

Table 5: Error Results of BP Neural Network Model

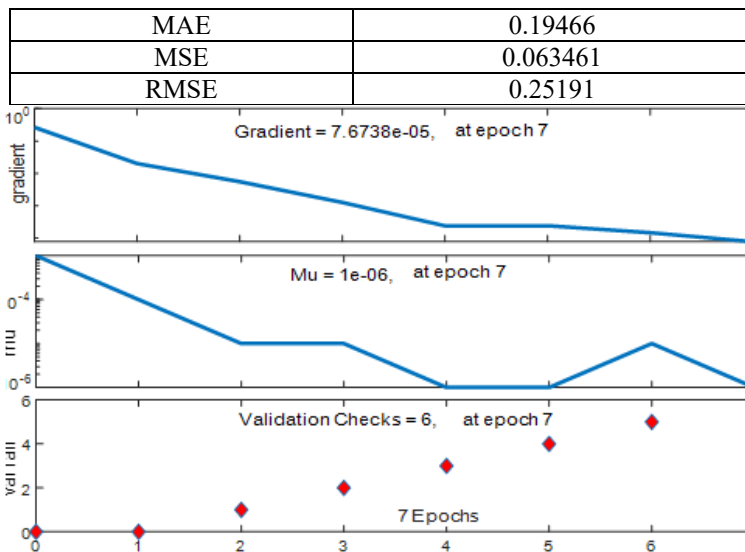


Figure 11: BP neural network training chart for predicting mean temperature at each stage

From Table 5, it can be seen that the errors are all within the credible range, so the BP neural network model can be used for statistics and prediction of global average temperature. The analysis results of global average temperature based on BP neural network in the training set, validation set, and testing set stages are as follows (Figure 11).

With the gradual change of training times, the overall Mean squared error change of global average temperature is analyzed using BP neural network as follows (Figure 12).

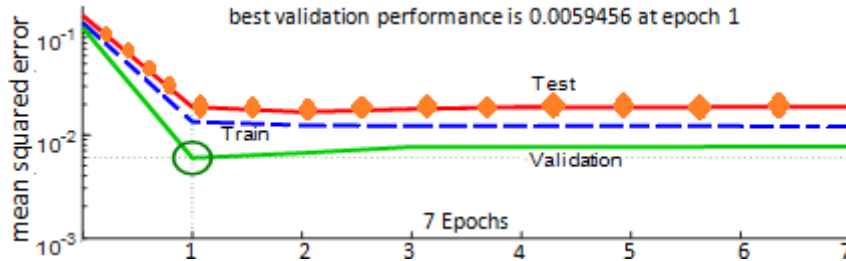


Figure 12: Mean squared error change of BP neural network predicted mean temperature

The BP neural network model has a good explanatory effect on predicting global temperature changes, and it is preliminarily predicted that the global average temperature will reach and maintain around 15.7881 °C from 2050 to 2100.

5.3 Global average temperature prediction based on ELMAN feedback neural network

One advantage of the ELMAN feedback neural network prediction model is that it can continuously update the next prediction data based on the obtained prediction data. The prediction model can be divided into four layers: input layer, hidden layer (middle layer), adapter layer, and output layer. Its characteristic is that the output of the hidden layer can be self-connected to the input of the hidden layer by taking on the delay and storage of the layer. This self-connection method makes it highly sensitive to historical state data. The addition of internal feedback networks enhances the network's ability to process dynamic information, thereby achieving the goal of dynamic modeling and prediction^[14].

When analyzing and predicting global average temperature based on the ELMAN feedback network model, the following settings must also be made in the training interface of Matlab software: (a) Divide the sample data into random partitions^[15]; (b) When training sample data, use the Gradient Descent with Momentum & Adaptive LR algorithm; (c) Mean squared error is used to measure network performance; (d) Set the target accuracy to 0.001.

The analysis results of the global average temperature prediction based on ELMAN feedback neural network at various stages of training, validation, and testing are as follows (Figure 13).

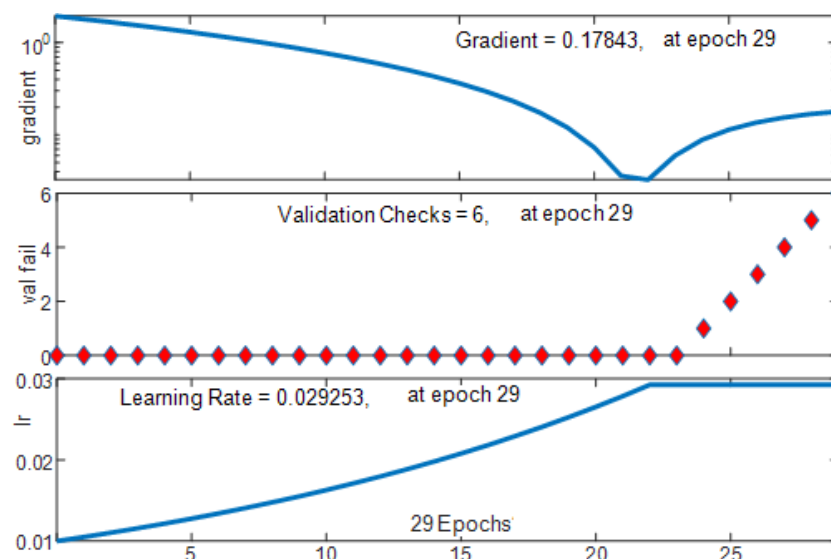


Figure 13: ELMAN feedback neural network training chart for predicting mean temperature at each stage

With the gradual change of training times, the overall Mean squared error change of global average temperature prediction based on ELMAN feedback neural network analysis is as follows (Figure 14).



Figure 14: Mean squared error change of ELMAN feedback neural network predicted mean temperature

Furthermore, to test the accuracy of the prediction, the predicted global annual average temperature based on ELMAN feedback neural network was compared with the actual values during the same period^[16], and the comparison results are as follows (Figure 15).

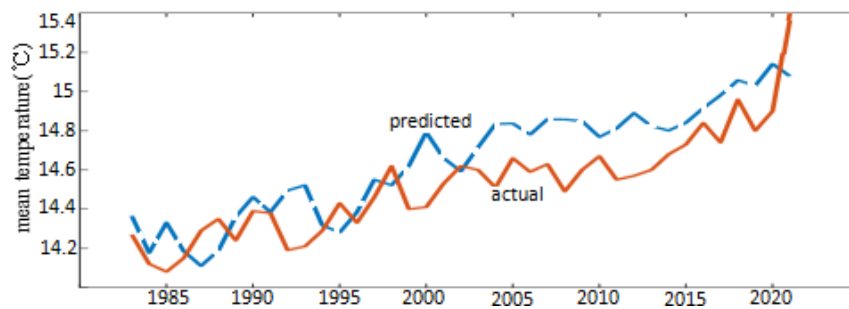


Figure 15: Comparison between actual and predicted annual average temperature based on ELMAN neural network model

In summary, we believe that the ELMAN neural network model has good accuracy in predicting global temperature changes, and ultimately predicts a global average temperature of approximately 16.6433°C from 2050 to 2100.

5.4 Comparison

Comparing the stability of BP neural network model and ELMAN feedback neural network model in temperature prediction, we found that the latter has more accurate prediction results, for the following reasons: under the condition that the target accuracy is set to 0.001 and the number of training samples is equal, the prediction process and results of the ELMAN feedback neural network model and the standard BP neural network model on the training samples are compared as follows (Table 6)^[17].

Table 6: Comparison of ELMAN and BP prediction processes and results for training samples

| type of network | target accuracy | convergence steps | Convergence time | mean squared error |
|-----------------|-----------------|-------------------|------------------|--------------------|
| ELMAN | 0.001 | 18 | 0.87 | 0.00013731 |
| BP | 0.001 | 17885 | 32.02 | 0.00099995 |

It can be seen from Table 6 that under the same target accuracy, the convergence steps and time of BP neural network are far greater than those required by ELMAN neural network, and the Mean squared error of the former is also far greater than the latter. Therefore, for the training sample set, only the training deployment is set sufficiently large, and the convergence time, Mean squared error, and convergence steps of the ELMAN neural network model are smaller than those of the BP neural network model^[18].

In conclusion, in terms of temperature prediction, compared with BP neural network model, ELMAN neural network model has higher accuracy and precision for training samples and faster Rate of convergence, so ELMAN neural network model has better prediction effect.

6. Conclusion

This article mainly studies the spatiotemporal average temperature changes in different temperature zones around the world, and predicts global temperature changes from the next 30 to 80 years by establishing BP neural network models and ELMAN neural network models. The predicted results are as follows: Firstly, the global average temperature has shown a significant upward trend since 1950, and the frequency of extreme weather events is also increasing; Secondly, there is a warming trend in the southern temperate zone, southern tropical zone, northern temperate zone, and northern tropical zone, but the temperature change trend is stable, and extreme weather mostly occurs in the mid to late 20th century; Thirdly, the BP neural network is used to predict that the global average temperature will reach a peak of 15.7881°C around 2050, while the ELMAN neural network is used to predict that the global average temperature will also reach a peak of 16.6433°C around 2050, and the global average temperature will remain unchanged until 2100; Finally, in predicting global average temperature, the ELMAN neural network prediction model outperforms the BP neural network prediction model in all aspects.

References

- [1] Deswal S, Pal M. (2008). *Artificial neural network based modeling of evaporation losses in reservoirs. International Journal of Mathematical, Physical and Engineering Sciences*, 2(4), 177-181.
- [2] Elsken T. (1997). *Even on finite test sets smaller nets may perform better. Neural Networks*, 10(2), 369-385.
- [3] Hamid Taghavifar, Aref Mardani, Ashkan Haji Hosseinloo (2015). *Appraisal of artificial neuralnetwork-genetic algorithm based model for prediction of the power provided by the agricultural tractors. Computational Intelligence and Bio inspired systems*, 93, 1704-1710.
- [4] Hong Y, Hsu K, Sorooshian S, et al. (2004). *Precipitation estimation from remotely sensed imagery using an artificial neural network cloud classification system. Journal of Applied Meteorology*, 43(12), 1834-1853.
- [5] Hou Huiqing (2021). *Global Climate Change Prediction Model Based on BP Neural Network. Science and Technology and Innovation*, 9, 10-11.
- [6] Hsieh W W, Tang B. (1998). *Applying neural network models to prediction and data analysis in meteorology and oceanography. Bulletin of the American Meteorological Society*, 79(9), 1855-1870.
- [7] Wang, Jidong, Ran Ran, and Yue Zhou (2017). *A Short-Term Photovoltaic Power Prediction Model Based on an FOS-ELM Algorithm. Applied Sciences*, 7(4), 423.
- [8] Jin Long, Chen Ning, Lin Zhenshan (1999). *Study and comparison of ensemble forecasting based on artificial neural network. Acta Meteorologica sinica*, 57(2), 198-207.
- [9] Kodogiannis VS, Amina M. (2013). *Petrounias I. A Clustering-based Fuzzy Wavelet Neural Network Model for Short-term Load Forecasting. International Journal of Neural Systems*, 23(5), 135-139.
- [10] Li Guoyong (2010). *Intelligent Predictive Control and Its MATLAB Implementation. Beijing: Electronic Industry Press*, 16-24.
- [11] Lin Chan, Wang Qifeng, Zhu Liangshan (2013). *Calculation model of Wet-bulb temperature based on LM-BP neural network. Hydropower Energy Science*, 31 (1), 164-166.
- [12] Liu Zelin, Peng Changhui, Xiang Wenhua, et al. (2010). *Application of artificial neural networks in global climate change and ecology. Science Bulletin*, 55 (31), 2987-2997.
- [13] McCann D. (1992). *A neural network short term forecast of significant thunderstorms. Weather and Forecasting*, 7, 525-534.
- [14] M. Fagiani, S. Squartini, L. Gabrielli, et al. (2015). *A review of datasets and load forecasting techniques for smart natural gas and water grids: Analysis and experiments. Neurocomputing*, 170, 448-465.
- [15] Valverde Ramirez M C, de Campos Velho H F, Ferreira N J. (2005). *Artificial neural network technique for rainfall forecasting applied to the Sao Paulo region. Journal of Hydrology*, 301(1/4), 146-162.
- [16] Wang Xuming, Zhang Jundong, Liu Yifan, Zhang Gang (2023). *ARIMA prediction model based on Elman neural network modification. Journal of Shanghai Maritime University*, 44 (2), 57-61+76.
- [17] Wei Haikun. (2005) *Theory and Method of Neural Network Structure Design. Beijing: Arms industry Press*, 105-108.
- [18] Zhang Sai, Liao Shunbao (2011). *Simulation analysis of spatialized BP neural network model of multi-year average temperature. Journal of Earth Information science*, 13 (4), 534-538.